Elsevier Editorial System(tm) for International Journal of Refractory Metals and Hard Materials
Manuscript Draft

Manuscript Number: IJRMHM-D-14-00269

Title: FRACTURE TOUGHNESS OF CEMENTED CARBIDES: TESTING METHOD AND MICROSTRUCTURAL EFFECTS

Article Type: SI: Science of Hard Material

Keywords: Fracture Toughness; microstructural characterization

Corresponding Author: Mr. Saad Ahmed Sheikh, Masters

Corresponding Author's Institution: Chalmers University of Technology

First Author: Saad Ahmed Sheikh, Masters

Order of Authors: Saad Ahmed Sheikh, Masters; Rachid M'Saoubi , Dr.; Petr Flasar ; Martin Schwind , Dr.; Tomas Persson, Masters; Jing Yang ; Luis Llanes , Dr.

Abstract: Fracture toughness is one the most important parameters for design applications and performance assessment of cemented carbides. Different from hardness, fracture toughness is commonly a property more difficult to evaluate, particularly in brittle materials. A large number of different testing methods have been introduced to evaluate toughness of hardmetals, but in general all of them have either theoretically debatable issues or important experimental difficulties. In this study, three different fracture toughness testing methodologies are investigated: three-point bending on Chevron notched specimen ("reference" baseline), Palmqvist indentation test, and Hertzian indentation method. The work is conducted in several cemented carbide grades with different microstructures, in terms of both WC grain size and Co binder content. Aiming to have a comprehensive view of fracture toughness - microstructure relationship, the mechanical study is complemented by an accurate microstructural characterization; and experimental findings are finally analyzed and discussed on the basis of two theoretical models proposed in the literature.

***Highlights (for review)**

FRACTURE TOUGHNESS OF CEMENTED CARBIDES: TESTING METHOD AND MICROSTRUCTURAL EFFECTS

Highlights:

- Microstructural characterization is carried out using EBSD for nine different cemented carbide grades with varying grain size and cobalt content.
- Fracture toughness is determined using three different methods, and a comparison has been tried to establish between true fracture toughness ("reference") baseline method and results obtained from two different Indentation methods.
- Microstructural parameters obtained from EBSD are correlated to basic mechanical properties with much focus on fracture toughness.
- Theoretical fracture toughness models which utilize microstructural parameter details for each grade is also utilized and compared with the true fracture toughness for a wide range of binder composition and grain size of hardmetals.

FRACTURE TOUGHNESS OF CEMENTED CARBIDES: TESTING METHOD AND MICROSTRUCTURAL EFFECTS

Saad Sheikh [1, 2], Rachid M'Saoubi [1], Petr Flasar [3], Martin Schwind [1], Tomas Persson[1], Jing Yang [4], and Luis Llanes [4]

[1] Seco Tools AB, R&D Material and Technology Development, Fagersta, 73782, Sweden
[2] Surface and Microstructure Engineering, Dept. of Materials and Manufacturing Technology, Chalmers University of Technology, 41296, Sweden
[3] Pramet Tools, s.r.o., Czech Republic
[4] CIEFMA- Universitat Politècnica de Catalunya, Dept. of Materials Science and Metallurgical Engineering, Avda. Diagonal 647, Barcelona 08028, Spain

(1,2) saad.sheikh@chalmers.se (1) rachid.msaoubi@secotools.com
(3) petr.flasar@pramet.com
(1) martin.schwind@secotools.com (1) tomas.persson@secotools.com
(4) jing.yang1@upc.edu (4) luis.miguel.llanes@upc.edu

Abstract

Fracture toughness is one the most important parameters for design applications and performance assessment of cemented carbides. Different from hardness, fracture toughness is commonly a property more difficult to evaluate, particularly in brittle materials. A large number of different testing methods have been introduced to evaluate toughness of hardmetals, but in general all of them have either theoretically debatable issues or important experimental difficulties. In this study, three different fracture toughness testing methodologies are investigated: three-point bending on Chevron notched specimen ("reference" baseline), Palmqvist indentation test, and Hertzian indentation method. The work is conducted in several cemented carbide grades with different microstructures, in terms of both WC grain size and Co binder content. Aiming to have a comprehensive view of fracture toughness – microstructure relationship, the mechanical study is complemented by an accurate microstructural characterization; and experimental findings are finally analyzed and discussed on the basis of two theoretical models proposed in the literature.

1 Introduction

WC-Co cemented carbides, also referred to as hardmetals, exhibit an excellent combination of mechanical properties. This is the main reason for its successful implementation as tool materials in a wide range of applications: metal cutting, mining, machining and metal forming, among others [1]. Among these properties, fracture toughness is one the most important parameters for design applications and performance assessment of cemented carbides. Keeping fair toughness and maximizing hardness are prime concerns of hardmetal industry. However, different from hardness, fracture toughness is commonly a property more difficult to evaluate, particularly in brittle materials. In this regard, a large number of different testing methods have been introduced to evaluate toughness of hardmetals: Palmqvist indentation method, impact strength test on plane or notched bars, fracture mechanics protocols using either notched (Chevron or V-notch) or precracked specimens, etc. (e.g. Refs. [2-7]). In general, all of them have either theoretically debatable issues or important experimental difficulties [7,8]. This is specifically true for approaches based on conventional fracture mechanics testing, where introduction of sharp and residual stress – free cracks into specimens are required.

Within the above framework, an effort is here proposed to evaluate different fracture toughness testing methodologies where above experimental limitations are avoided: three-point bending on Chevron notched specimen (e.g. Ref. [9]) as "reference" baseline, the practical Palmqvist indentation test, and Hertzian indentation method [10]. Different from the former two approaches, the use of the latter for assessing fracture toughness of cemented carbides has been quite limited [11], even though it has similar advantages offered by the Palmqvist method compared with the more conventional testing protocols, i.e. a straightforward experimental procedure, minimal specimen preparation, and small amount of needed material needed [10]. The systematic study attempted is conducted in several cemented carbide grades with different microstructures, in terms of both WC grain size and Co binder content. Aiming to have a comprehensive view of fracture toughness – microstructure relationship, the mechanical study is complemented by an accurate estimation of single- and two-phase microstructural parameters, i.e. carbide grain size and cobalt content, as well as cobalt binder mean free path and carbide contiguity, respectively. Finally, experimental findings are analyzed and discussed on the basis of two theoretical models proposed in the literature by other authors.

2 Materials and experimental methods

2.1 Materials and microstructural characterization

Nine different cemented carbides with varying grain size and cobalt content were manufactured for the experiments. The materials were consolidated by liquid phase sintering at temperatures in the range between 1390 °C and 1470 °C following the conventional powder metallurgy route. Nominal compositional details with varying cobalt binder content and carbide grain size for each hardmetal grade studied are listed in **Table 1**. Scanning electron microscopy (SEM) micrographs for four of the investigated materials are shown in **Figure 1**.

TABLE 1

FIGURE 1

Microstructure of WC-Co cemented carbides is usually characterized in terms of both single-phase parameters: carbide phase size (d) and cobalt volume fraction (V_{Co}), as well as two-phase ones: carbide contiguity (C) and binder mean free path (λ). These parameters have great influence on the overall properties of hardmetals. Carbide grain size and contiguity were determined by SEM and electron back scattered diffraction (EBSD) with an EBSD system manufactured by HKL using their Channel 5 software. To obtain high quality patterns for the EBSD analysis the specimens were mechanically polished with diamond slurry to 1 µm, followed by ion beam etching (Ar^+) in a JEOL cross section polisher (SM-09010) with 6 kV energy and approximately 1° incident angle. EBSD mapping was performed on a Zeiss Supra 40 high resolution SEM. Optimum step size was chosen in the range 0.06 - 0.15 µm depending on the carbide grain size. The specimens were tilted 70° using a 20 kV voltage at high current mode with 60 µm aperture. After refining the data from faulty indexing, by means of wild spikes correction and noise reduction, grain size maps were constructed. Once the refined maps are obtained, the area of each WC grain can be calculated. Carbide grains may be approximated as spherical, as recommended by Stjernberg *et al.* [12]; and thus, equivalent circle diameter can be used to describe the two dimensional WC grain size. The equivalent diameter for each individual detected grain can then be used for microstructural analysis. Further details on the EBSD characterization are described elsewhere [13-15].

After obtaining orientation maps, MATLAB software was utilized to determine the number of carbide / carbide (N_{cc}) and binder / carbide boundaries (N_{bc}) per unit length. Volume fraction of binder was also calculated using EBSD. On the basis of experimental data gathered, contiguity (C) and binder mean free path (λ) were determined according to [16,17]:

$$C = \frac{2N_{CC}}{\left(2N_{cc} + N_{bc} * \sqrt{(Vol.\%\ of\ binder\ theoretical\ /\ Vol.\%\ obtained\ from\ EBSD)}\right)} \quad (1)$$

and

$$\lambda = d * \frac{V_{Co}}{(1-V_{Co})(1-C)} \quad (2)$$

Microstructural data for the nine hardmetal grades investigated are listed in **Table 1**.

2.2 Fracture toughness

2.2.1 Chevron-notched three-point bending test

Advantages of toughness measurement of cemented carbides through three-point bending test of Chevron-notched specimens include no pre-cracking requirement and easy testing configuration. Within this context, values assessed following this testing procedure will be used, for comparison purposes, as "reference" baseline for further discussion on testing method and microstructural effects on fracture toughness. Rectangular bars of dimensions (53x3x4 mm^3), nine for each hardmetal grade, were manufactured. A Chevron notch was introduced in each specimen by means of electrical discharge machining. Thickness of the cutting wire was 0.15 mm. The Chevron notch angle (θ) was 90º while the tip of the notch was positioned at about 1 mm below the tensile surface. Specimens were broken under three-point bending, with a specimen span S of 16 mm. Tests were conducted in an Instron 8862 electro-mechanical testing device, with overall load capacity of 100kN. For measurement purposes, the device was instrumented with a 5 kN load cell. To be able to measure deflection of the testing sample, a LVDT displacement gauge was used during the test. The stress intensity factor for a Chevron notched specimen loaded in flexure under three-point bending can be expressed as [18-20]:

$$K_{Ic} = \frac{F_{max} Y^*_{min}}{B(W)^{1/2}} \quad (3)$$

where K_{Ic} is expressed as $MPam^{1/2}$, F_{max} is the maximum load and Y^{*}_{min} is a geometry factor dependent on a/W [21], where a is initial crack length and W (4 mm) is the height. Finally, B (3 mm) is the specimen width.

2.2.2 Palmqvist Indentation toughness

Palmqvist indentation toughness was determined on square shaped (12x12x5 mm^3) cemented carbide specimens. Ten indentations for each grade were carried out on diamond polished surfaces. A 0.75 mm distance between indentations was kept in order to avoid any overlapping effects. Indentation load (*P*) was 30 *kgf*, as recommended by ISO 3878 and lengths (*L*) of cracks starting at the corners of indentation were measured by light optical microscopy at 500X magnification. Palmqvist fracture toughness was assessed from Shetty et al.'s equation [22], according to:

$$K_{Ic} = A\sqrt{H}\left(\frac{P}{\Sigma L}\right) \qquad (3)$$

where H is the hardness (*N/mm²*), P is the applied load (*N*), ΣL is the sum of crack lengths (*mm*), A is a constant with value of 0.0028, and K_{Ic} is given as $MPam^{1/2}$. For $HV30$ values expressed in (*kgf/mm²*), Palmqvist fracture toughness can be calculated as:

$$K_{Ic} = 0.15\left(\frac{HV_{30}}{\Sigma L}\right) \qquad (4)$$

2.2.3 Hertzian Indentation toughness

Many attempts have been made to use Hertzian indentation – where a hard sphere is pressed into the flat surface of a brittle substrate - to determine fracture toughness of brittle materials [23-25]. In this study, early experimental limitations on the use of this technique are overcome by following the protocol proposed by Warren [10] which simply requires measurement of the fracture load. It is based on a refined stress intensity factor formulation for surface-breaking cracks in steep-stress gradients [26] which enables estimation of the minimum loads necessary to propagate cracks by Hertzian indentation. Thus, indentation tests on a flat surface of a brittle material, performed with a sphere of given radius *R* and made of the same material, allow measurement of a definite minimum load of fracture ($P_{F\ min}$), which is used for determining fracture toughness (K_{Ic}) according to:

$$K_{Ic} = \left(\frac{E^* P_{F\min}}{P_{FN}^{\min} R} \right)^{1/2} \qquad (5)$$

where E^* is the reduced “specimen+indenter” Young modulus, and $P_{FN}^{\min}$ is a normalized fracture load necessary to propagate short plane cracks of length c, located normal to the free surface and close to the contact zone of radius a.

At this stage, it should be highlighted that $P_{FN}^{\min}$ is a dimensionless quantity, exclusively dependent on the Poisson ratio (ν) of the material tested ($P_{FN}^{\min}$ values for ν range relevant for this study are: 2025, 2247 and 2490 for ν values of 0.21, 0.22 and 0.23 respectively). On the other hand, occurrence of such fracture (radial cracking) event requires propagation of pre-existing flaws. As a consequence, minimum normalized lengths $(c/a)_{min}$ corresponding to surface crack depths in the 5-10 μm range are required. It points out abrasion with fine SiC grits, instead of fine diamond polish, as recommended surface preparation method. However, such abrasion may introduce surface residual stresses, and this effect should be analysed too. Accordingly, two different surface conditions were investigated: one attained through abrasion using SiC 600 grit size, and another corresponding to final polishing using 6 micron diamond. After grinding and polishing, residual stress measurements were carried out using X-Ray diffraction analysis [27]. Residual stresses were determined in the WC phase in both parallel and transversal directions.

Regarding experimental issues, Hertzian indentation tests were conducted using spherical hardmetal indenters with two different radii i.e. 1.25 mm and 2.5 mm. After indentation, specimens were inspected with light optical microscope to discern cracking features at the imprint contour. Once the minimum load for cracking was assessed, fracture toughness was finally calculated using equation (5). Such a procedure was conducted for each surface condition and indenter radius in four selected hardmetal grades: A, C, H and I.

3. Results and discussion

3.1 Microstructural parameters obtained from EBSD and relation to basic mechanical properties

Mechanical properties of WC-Co composites are dependent on volume fraction of each phase and carbide grain size. As the volume fraction of the carbide phase increases, hardness rises and fracture toughness decreases. On the other hand, grades with fine carbides exhibit higher hardness and lower fracture toughness than those with a coarser microstructure. The combined effect of these single-phase parameters may be captured by means of two-phase microstructural parameters such as carbide contiguity and binder mean free path. In general, contiguity is observed to increase as carbide content rises and carbide grain size decreases. **Figure 2** shows EBSD orientation maps obtained. In such images, red and green boundaries correspond to WC-Co and WC-WC interfaces respectively.

FIGURE 2

Microstructural characteristics, including volume fraction of binder phase, determined from EBSD measurements are presented in Table 2. Values for basic mechanical properties: elastic modulus (E) and Poisson's ratio (ν), determined according to ASTM E1876-01, and hardness (HV30) are also listed in **Table 2**. As expected, hardness is discerned to decrease as binder mean free path rises (**Figure 3**).

TABLE 2

FIGURE 3

3.2 Fracture toughness - microstructure correlation

Chevron-notched three-point bending test is an efficient method for fracture toughness assessment of brittle cemented carbides. In this study, deflection was recorded by a linear variable differential transformer (LVDT) device and a typical force-deflection cuve is shown in **Figure 4**. At a critical crack length, the load required to propagate the crack passes through a maximum, and such value is then used for determining fracture toughness. Main advantage of this method is that it avoids any precracking requirement. The values obtained by using this testing method are here used as baseline and are thus referred as "reference" K_{Ic}. **Figures 5-7** display the variation of "reference" K_{Ic} as a function of hardness, carbide contiguity and binder mean free path, respectively. The results indicate a consistent decrease of fracture toughness with increasing hardness and carbide contiguity, and decreasing binder mean free path.

FIGURE 4

FIGURES 5-7

A comparison of the fracture toughness values obtained by the different testing methods investigated is shown in **Table 3**. For most of the hardmetal grades studied, a reasonably good agreement is found between K_{Ic} values obtained through Chevron-notched three-point bending test and Palmqvist indentation. It corresponds to a toughness range from 10 to 14 $MPam^{1/2}$. However, this was not the case for grade H which exhibits a relatively higher toughness level.

TABLE 3

Depending on indenter shape, three distinct indentation modes take place in brittle materials. Ring cracks and Hertzian cone cracks are formed when indenter is rounded while lateral vents or median vents are formed when the indenter is sharp. For the case of cemented carbides, median vents are formed in the underlying material and median vents are divided into two types: median cracks and Palmqvist cracks. Schematic of Palmqvist and median cracks are mentioned in detail elsewhere [28]. Crack geometry beneath indentation for grade A is shown in **Figure 8**. This was the cracking scenario discerned for most of the hardmetal grades studied. It clearly follows a Palmqvist crack geometry, a necessary condition for assessing fracture toughness through equation (3).

FIGURE 8

On the other hand, the combined effect of high binder content and relatively coarse carbides (e.g. H grade) results in a relevant departure from the brittle-like nature suitable for satisfying requirements implicit to application of indentation fracture mechanics [5,7]. For cemented carbide H, a well-defined cracking system (with long enough fissures, as compared to indentation impression size) is not developed at the corners of Vicker's indentations, even if applied load is risen up to 100 kgf. Moreover, increasing the load above 30 kgf also implies a damage or failure risk for the indenter. **Figure 9** shows indentation imprints and induced cracks (under same indentation load) for materials C and H, grades with similar cobalt binder content but different carbide grain size. Looking at the cracking system generated in the H grade, it is evident that some of the hypothesis assumed in developing relationships like Shetty et al.'s equation, based on an approximate fracture mechanics analysis [22], are not valid for relatively tough (above 14 $MPam^{1/2}$) hardmetals. As a consequence, toughness assessed from Shetty et al.'s equation in those materials yield overestimated values.

FIGURE 9

Regarding toughness assessment by means of Hertzian indentation (using an indenter of radius 1.5 mm and surface finish resulting from final polishing using 6 micron diamond), it seems to yield overestimated values for the two fine-grained grades tested (i.e. A and D materials). On the other hand, it results in quite concordant values, as compared to those measured by means of the reference Chevron-notched three-point bending test, for the medium/coarse grained grades (i.e. H and I).

Aiming for a deeper study on the implementation of Hertzian indentation methodology, use of indenters with different radii and surface conditions (abraded with SiC 600 grit size and polished with 6 micron diamond) were tested. Ring cracks formed at the surface of grade C, at applied critical load using the 2.5 mm radius indenter, for the two referred surface conditions are shown in **Figure 10**. Furthermore, as surface residual stresses were expected to be introduced through abrasion with SiC 600 grit size, they were measured on two different surfaces, parallel and transverse directions [27]. The results obtained are shown in **Table 4**. It is evident that compressive residual stresses are much higher for abraded specimens than for polished ones. However, and very interesting, they are higher for the harder grades. The effect of different surface treatments (and residual stresses) along with varying spherical indenter radii (r_e) on fracture toughness is shown in **Table 5**. The higher toughness values determined for abraded specimens, as compared to the polished ones under similar testing conditions, are intimately related to the compressive residual stresses induced during surface preparation in the former.

FIGURE 10

TABLE 4

TABLE 5

In order to obtain the appropriate toughness values through Hertzian indentation using spheres with radii between 1 and 5 mm, preexisting flaws of length between 5 and 10 μm are required. Accordingly, a relatively coarse surface texture is required. However, mechanical treatment of surfaces for attaining such rough-like profile, usually result in relevant surface residual stresses (e.g. **Table 4**); which may then result in overestimated fracture toughness values. Even if residual stresses are disregarded, an intrinsic overestimation should also be expected, as the flaw density is not infinite in reality, and cracks will not be situated at the particular position for which critical stress intensity factor is minimum. Beyond these experimental limitations, it should also be highlighted the main advantage of using this method: it does not require any measurement of radius of ring-crack and there is no need to determine initial crack size.

Following the above findings, from a practical view it is finally interesting to evaluate the particular measurement reliability of each method as a function of a basic mechanical property such as hardness. In this regard, Chevron-notched three-point bending test yields reliable fracture toughness values for a wide range of cemented carbide grades with varying hardness. Concerning indentation methods, the Hertzian one may be particularly recommended, as compared to Palmqvist method, as far as hardness (HV30) drops below 1300. On the other hand, if HV is higher than 1300; results estimated from Shetty et al.'s equation may be taken as reliable for assessment of fracture toughness.

3.3. Theoretical considerations

Based on different microstructural parameters and assuming deformation in cobalt binder and carbides, different fracture toughness models have been proposed in the past. Using these microstructural parameters, an effort is here carried out to evaluate how experimental data here gathered fit within estimations extracted from two specific models.

3.3.1 Godse and Gurland's model (GGM) [29]

This model uses the idea of ductile fracture proposed by Rice and Johnson [30], i.e. a critical strain should be exceeded for crack growth to take place. Fracture toughness obtained using this model is based on the fact that crack growth resistance comes from the ductile binder (cobalt) and is valid for 10 % to 25% binder volume fraction.

Fracture toughness K_{Ic} may be estimated from equation (9):

$$K_{IC} = \sqrt{R(\lambda + d)E'\sigma_B \frac{(1 - CV_{WC})}{C_1}} \qquad (9)$$

where C, d and V_{WC} are the contiguity, grain size and volume fraction of the carbide phase respectively; λ is the binder mean free path; R is a floating parameter calculated on the basis of best fitting with experimental data [29], C_1 is taken from Mcmeeking's work [31] as 0.54, E' can be calculated by using equation (10) for plane stress:

$$E' = \frac{E}{1-U^2} \qquad (11)$$

and σ_B is the binder effective flow stress, calculated by using equation (12) as proposed by Sigl and Fischmeister [6]:

$$\sigma_B = 480 + \frac{1550}{\lambda}[MPa] \qquad (12)$$

3.2 Ravichandran's model (RM)

Ravichandran [32] proposed evaluation of the strain energy release rate (G_C) as the sum of fracture resistance of binder phase and fracture energy of carbide phase according to equation (13):

$$G_C = (1-V_f)G_m + V_f \sigma_O h \chi \qquad (13)$$

where G_m is the strain energy release rate of the brittle WC phase, h is similar as binder mean free path (λ), V_f and σ_O are volume fraction and bulk flow stress of binder. χ is defined as the work of rupture and is related to bulk flow stress of the binder as follows:

$$\chi = \sigma_{eff} \frac{\beta}{\sigma_O} \qquad (14)$$

and bulk flow stress of the binder may be further elaborated using by relating it to effective flow stress σ_{eff} , according to:

$$\frac{\sigma_{eff}}{\sigma_O} = \left[1 + \frac{2k}{3}\left(\frac{d}{2h}\right)\right] \qquad (15)$$

where d is the carbide grain size and k is the maximum shear factor with a value of 0.577.

As a final outcome, fracture toughness can be determined by the following relation (16):

$$K_C = \sqrt{\frac{E_C (1-v_m^2)(1-V_f)K_m^2}{(1-v_C^2)E_m} + \frac{\beta V_f E_C \sigma_{eff} h}{(1-v_C^2)}} \qquad (16)$$

where K_C is the fracture toughness of the WC-Co composite, E_C and v_C are elastic modulus and Poisson's ratio of the composite, β is a constant with value 2, and may is defined as the ratio of critical crack tip to binder thickness; K_m, E_m and v_m are fracture toughness, elastic modulus and Poisson's ratio of the brittle WC phase.

3.3.3. Fitting of experimental data to the models under consideration

A comparison between the "reference" K_{Ic} values and estimations resulting from the above theoretical models are presented in **Table 6**. Both theoretical models utilize different binder flow stress and this is something that needs to be further explored. For instance, RM considers a binder flow stress of 850 MPa, which is lower than the binder flow stress proposed in GGM. On the other hand, GGM requires modification of fitting parameters. As a result, it seems to overestimate the experimental values attained in this study. RM utilizes β=2, corresponding to a critical crack tip opening displacement at fracture twice the cobalt binder thickness. A slight modification of this parameter (β=1.1), indicative of an almost one-to-one relationship between critical crack tip opening displacement at fracture and binder thickness yields the best fitting of the experimental data. Further exploitation and adjustment may be done in order to have better estimations from these models.

TABLE 6

6. Conclusions

- Chevron-notch three-point bending test may be taken as "reference" baseline method for determining the fracture toughness for a wide range of binder composition and grain size of hardmetals. Palmqvist method gives a good approximation of toughness for brittle-like cemented carbides, but becomes invalid for grades whose "reference" toughness is higher than 14 $MPam^{1/2}$. Regarding spherical indentation, optimum indenter radius along with flat surface, free from residual stresses, are important for the determination of fracture toughness. Hertzian indentation may result in overestimated values, this discrepancy becoming significant as hardness of the hardmetal increases.

- Current fracture toughness models overestimates the experimental "reference" fracture toughness values determined in this study. Slight modifications on fitting parameters associated with intrinsic uncertainties (binder flow stress, critical crack tip opening displacement at fracture, etc.) results in satisfactory agreement between experimental and estimated values.

References

[1] Prakash L. Introduction to hardmetals - Fundamentals and general applications of hardmetals. In: Mari D, Llanes L, Sarin VK, eds. Comprehensive Hard Materials, Vol. 1: Hardmetals. Elsevier; 2014. p. 29-90

[2] Exner HE, Walter A, Pabst R. Zur ermittlung und darstellung der fehlerverteilungen von spröden werkstoffen. Mater Sci Eng 1974; 16: 231-8

[3] Pickens JR, Gurland J. The fracture toughness of WC-Co alloys measured on single-edge notched beam specimens precracked by electron discharge machining. Mater Sci Eng 1978; 33: 135-42

[4] Viswanadham RK, Sun TS, Drake EF, Peck JA. Quantitative fractography of WC-Co cermets by Auger spectroscopy. J Mater Sci 1981; 16: 1029-38

[5] Shetty DK, Wright IG, Mincer PN, Clauer AH. Indentation fracture of WC-Co cermets. J Mater Sci 1985; 20: 1873-82

[6] Sigl LS, Fischmeister HF. On the fracture toughness of cemented carbides. Acta Metall 1988; 36: 887-97

[7] Torres Y, Casellas D, Anglada M, Llanes L. Fracture toughness evaluation of hardmetals: influence of testing procedure. Int J Refract Met Hard Mater 2001; 19: 27–34

[8] Roebuck B, Gee MG, Morrell R. Developments in testing and mechanical properties of hard materials. Powder Metall 1996; 39: 213-8

[9] Sakai M, Bradt RC. Fracture toughness testing of brittle materials. Int Mater Rev 1993; 38: 53-78

[10] Warren PD. Determining the fracture toughness of brittle materials by Hertzian indentation. J Eur Ceram Soc 1995; 15: 201-7

[11] Laugier MT. Hertzian indentation of ultra-fine grain size WC-Co composites. J Mater Sci Lett 1987; 6: 841-3

[12] Stjernberg KG. Determination of volume distribution function by lineal analysis, Chalmers University of Technology, Gothenburg, Sweden; 1969

[13] Humphreys FJ. Grain and sub grain characterization by electron backscatter diffraction. J Mater Sci 2001; 36: 3833-54

[14] Randle V, Microtexture determination and its applications. 2nd ed. London: Institute of Materials / Maney; 2003

[15] Mingard KP, Roebuck B, Bennett EG, Gee MG, Nordenstrom H, Sweetman G, Chan P. Comparison of EBSD and conventional methods of grain size measurement of hardmetals. Int J Refract Met Hard Mater 2009; 27, 213-22

[16] Roebuck B, Bennett EG. Phase size distribution in WC/Co hardmetal. Metallography 1986; 19: 27-47

[17] Xu Z-H, Ågren J. A modified hardness model for WC–Co cemented carbides. Mater Sci Eng 2004; A386, 262-8

[18] Barker LM. Theory for determining K_I, from small, non-LEFM specimens, supported by experiments on aluminum. Int J Fract 1979; 15, 515-36

[19] Munz D, Bubsey RT, Srawley JE. Compliance and stress intensity coefficient for short bar specimens with chevron notches. Int J Fract 1980; 16, 359-74

[20] Deng X, Bitler J, Chawla KK, Patterson BR. Toughness measurement of cemented carbides with Chevron-notched three-point bend test. Adv Eng Mater 2010; 12, 948-52

[21] Biner SB, Barnby JT, Elwell DWJ. On the use of short-rod / bar test specimens to determine the fracture toughness of metallic materials. Int J Fracture 1984; 26: 3-16

[22] Shetty DK, Wright IG, Mincer PN, Clauer AH. Indentation fracture of WC-Co cermets. J Mater Sci 1985; 20: 1873-82

[23] Frank FC, Lawn BR. On the theory of Hertzian fracture. Proc R Soc Lond 1967; A229: 291-306

[24] Wilshaw TR. The Hertzian fracture test. J Phys D: Appl Phys 1971; 4: 1567-81

[25] Franco Jr A, Roberts SG. Surface mechanical analyses by Hertzian indentation. Cerâmica 2004; 50: 94-108

[26] Warren PD, Hills DA, Roberts SG. Surface flaw distributions in brittle materials and Hertzian fracture. J Mater Res 1994; 9: 3194-202

[27] Larsson C, Odén M. X-ray diffraction determination of residual stresses in functionally graded WC–Co composites. Int J Refract Met Hard Mater 2004; 22: 177-84

[28] Spiegler R, Schmauder S , Sigl LS. Fracture toughness evaluation of WC-Co alloys by indentation testing. J Hard Mater 1990; 1: 147-58

[29] Godse R, Gurland J. Applicability of the critical strain fracture criterion to WC-Co hardmetals. Mater Sci Eng 1988; A105/106; 331-6

[30] Rice JR, Johnson MA. Inelastic behavior of solids . In Kanninen MF, Adler WF, Rosenfield AR, Jaffe RI (eds.). McGraw-Hill, New York, 1970

[31] Mcmeeking, RM. Finite deformation analysis of crack-tip opening in elastic-plastic materials and implications for fracture. J Mech Phys Solids 1977; 25: 357-81.

[32] Ravichandran KS. Fracture toughness of two phase WC-Co cermets. Acta metal mater 1994; 42: 143-50.

List of Figures

List of Tables

FIGURES DETAILS

FIGURE 1

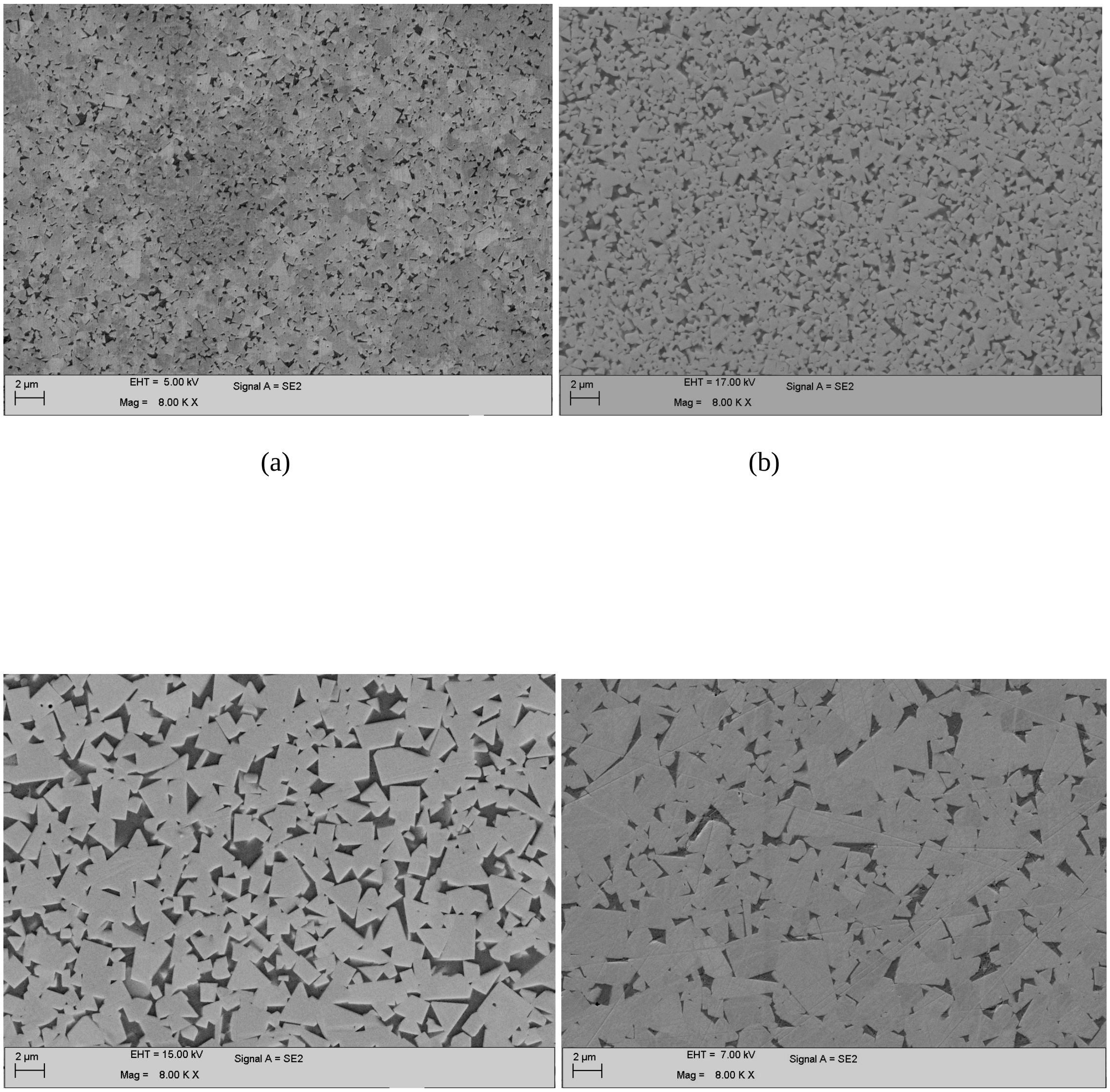

(a) (b)

(c) (d)

Figure 1: SEM images of (a) grade A, (b) grade C, (c) grade H and (d) grade I

FIGURE 2

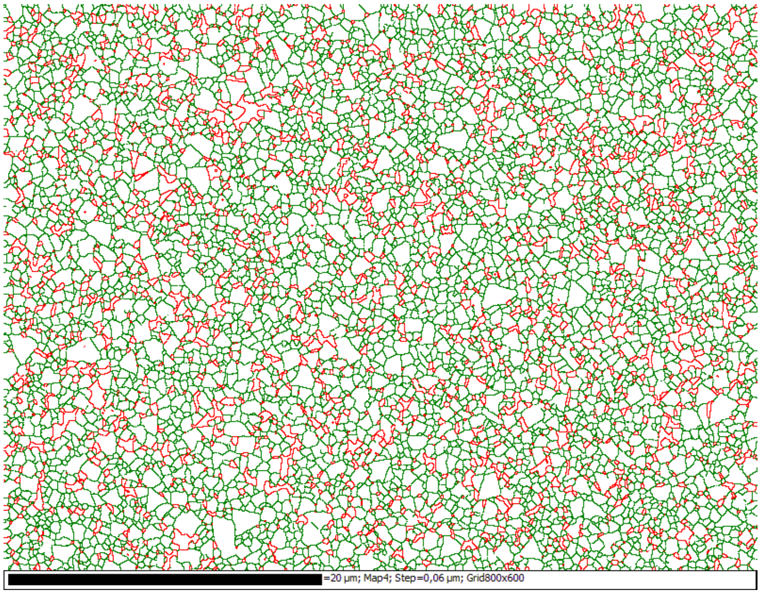

Figure 3: EBSD orientation maps after noise reduction for grade A in which WC-Co interfaces are red while WC-WC interfaces are green

FIGURE 3

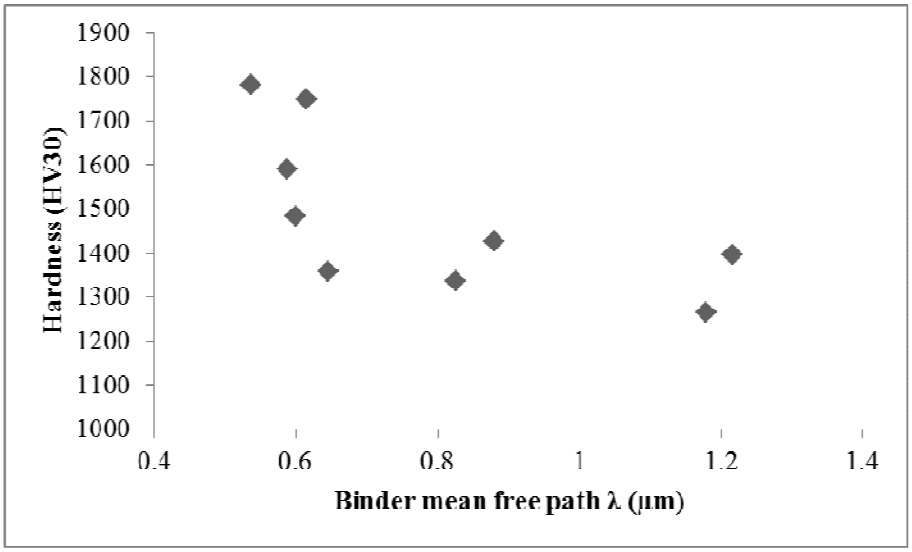

Figure 3: Hardness variation with increase in binder mean free path

FIGURE 4

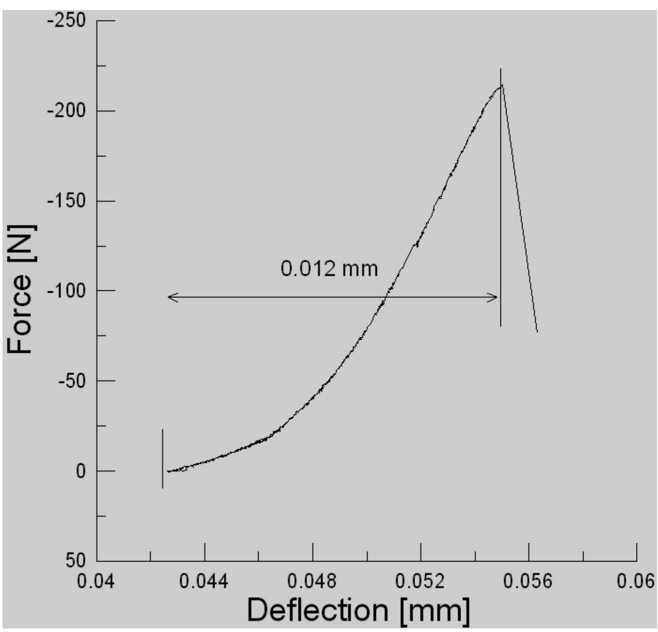

Figure 4: Force deflection curve of grade B for Chevron-notched specimen

FIGURE 5-6

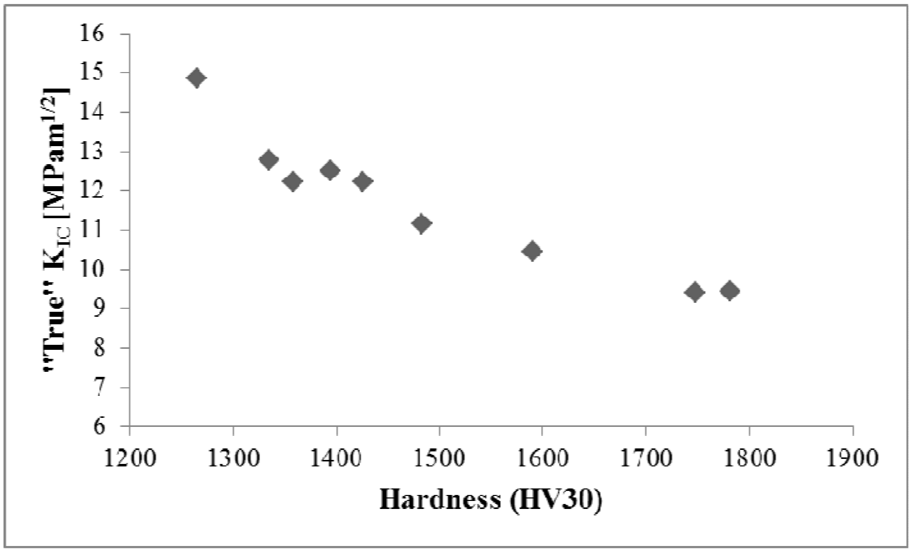

Figure 5: K_{IC} vs Hardness

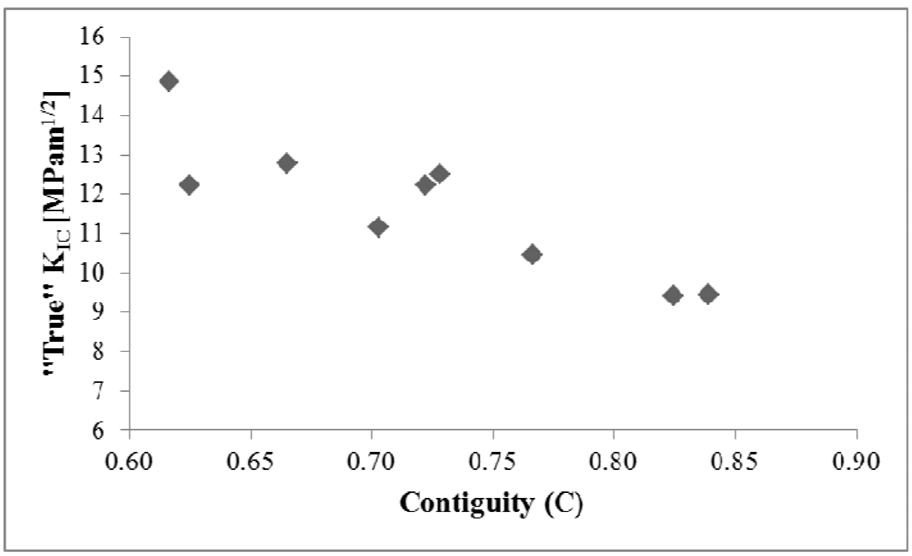

Figure 6: K_{IC} vs Contiguity

FIGURE 7

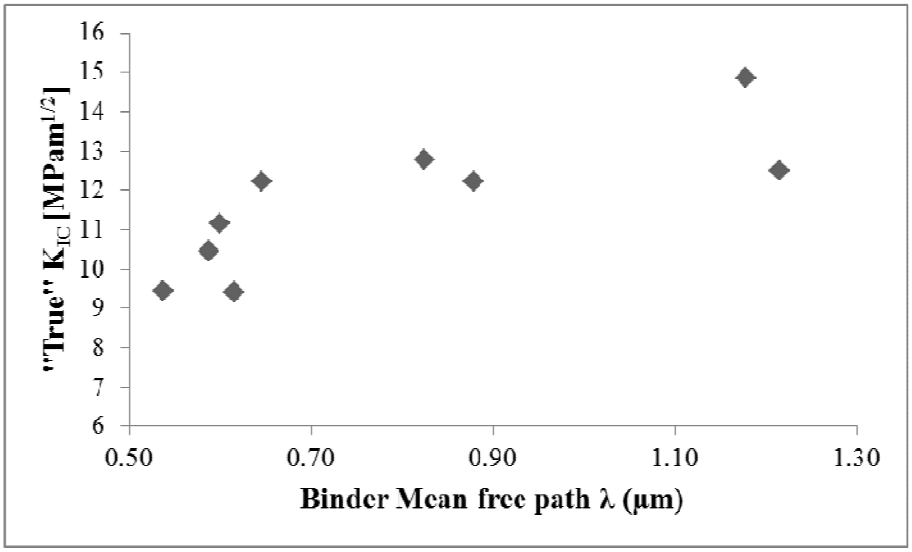

Figure 7: K_{IC} vs binder mean free path

FIGURE 8

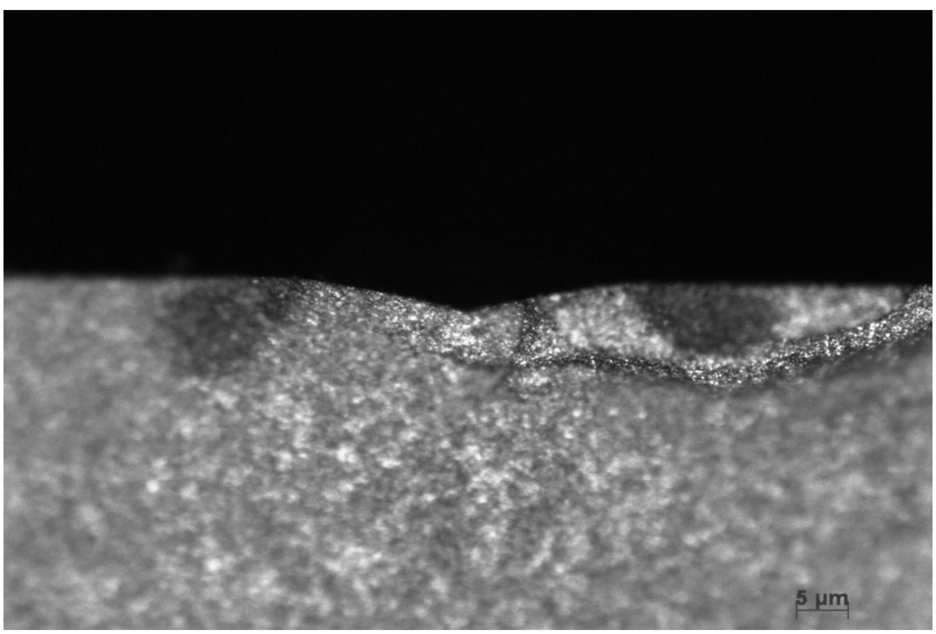

Figure 8: Palmqvist cracks geometry beneath indentation for grade A

FIGURE 9

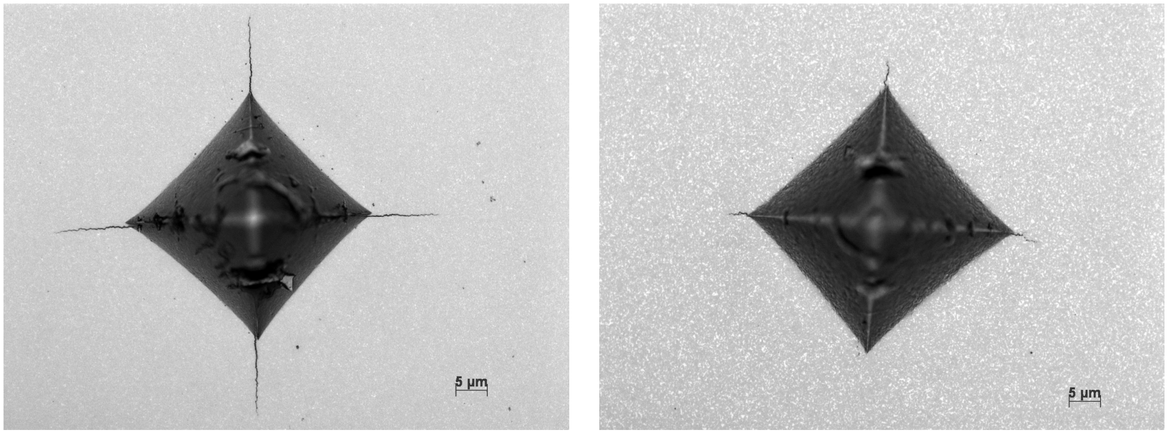

(a) (b)

Figure 9: Vicker's Indentations formed on the surface of grade C and grade H

FIGURE 10

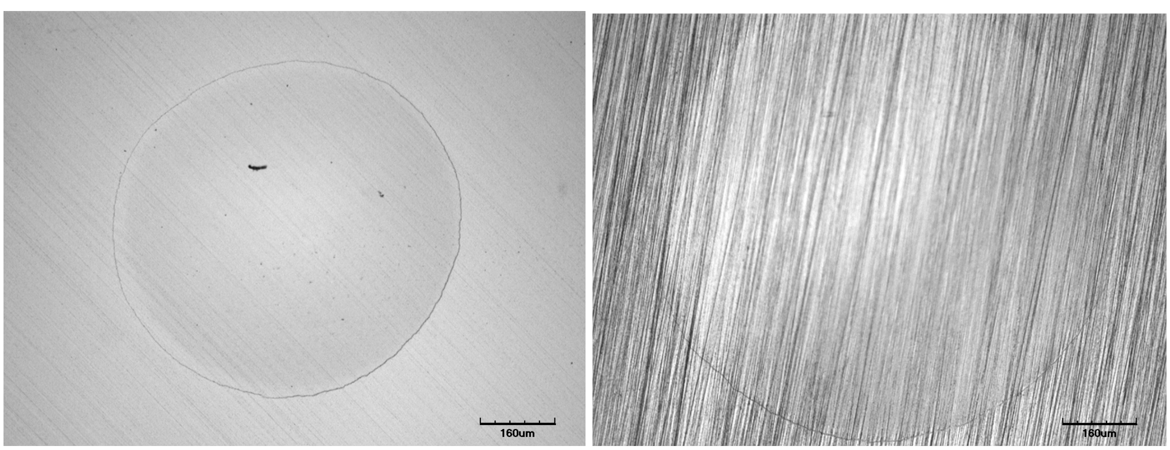

(a) (b)

Figure 10: Surface ring cracks for grade C with $2.5\ mm$ indenter radius for 6 micron (a) and SiC 600 (b)

TABLES DETAILS

TABLE 1

Grade	Vol. % - Co (Theor.)	Grain size d (μm)
A	11	0.7
B	17	0.7
C	21	0.7
D	12	0.8
E	20	1
F	14	1.5
G	17	1.4
H	21	1.7
I	13	2.2

Table 1: Nominal compositional detail and grain size of each cemented carbide grade.

TABLE 2

Grade	$N_{wc/wc}$	$N_{wc/co}$	Vol. % -Co EBSD	Vol. % - Co (Theor.)	Contiguity (C)	d (μm)	λ (μm)	Hardness (HV30)	E (GPa)	ν	TRS (MPa)
A	101001	23898	4.2	11	0.84	0.7	0.54	1782	678	0.22	3130
B	89787	42043	10	17	0.77	0.67	0.59	1591	619	0.22	3655
C	76237	55491	15.6	21	0.70	0.67	0.60	1483	599	0.22	3833
D	106697	35855	7.5	12	0.82	0.79	0.61	1748	690	0.21	2129
E	46602	54202	18.8	20	0.62	0.97	0.65	1359	600	0.23	2858
F	67551	47822	11.9	14	0.72	1.5	0.88	1426	649	0.23	2486
G	64137	63832	16.6	17	0.67	1.35	0.83	1335	625	0.23	2885
H	62623	80272	22.3	21	0.62	1.7	1.18	1264	579	0.22	2904
I	74388	46303	9.1	13	0.73	2.21	1.22	1395	600	0.21	2416

Table 1: Composition, microstructural parameters and mechanical properties of each cemented carbide grade

TABLE 3

Grade	True K_{IC} (MPam$^{1/2}$)	Ind. Toughness Palmqvist (MNm$^{-3/2}$)	K_{IC} Hertzian Ind. (MPam$^{1/2}$)
A	9.44	9.39	11.70
B	10.44	10.97	
C	11.15	12.26	14.50
D	9.42	9.18	
E	12.23	13.55	
F	12.21	11.83	
G	12.79	13.75	
H	14.86	20.81	15.10
I	12.5	12.02	12.10

Table 3: Fracture toughness values obtained from Chevron Notched (True), Palmqvist toughness and Hertzian indentation ($1.5\ mm$ indenter radius and 6 Micron surface treated)

TABLE 4

Grade	Residual stresses (parallel direction) (MPa)	Residual stresses (transverse direction) (MPa)	Surface condition
A	-305 ± 37	-253 ± 23	6 micron
C	-325 ± 38	-395± 36	6 micron
H	-435± 32	-399±28	6 micron
I	-311±38	-332±24	6 micron
A	-3384 ± 104	-2966 ± 64	SiC grinded
C	-2577 ± 87	-2569± 103	SiC grinded
H	-1985± 49	-1984±76	SiC grinded
I	-2014±44	-2132±79	SiC grinded

Table 4: Residual stress measurements for 6 micron diamond polished and SiC grinded specimens.

TABLE 5

Grade	Surface Treatment	E^* (GPa)	$P_{f\,\min}$ (N)	$P_{FN}^{\min}$	r_e (mm)	K_{IC} (MPam$^{1/2}$)
A	6 Micron	360	3816	2247	2.5	15.7
C	6 Micron	338	4186	2247	2.5	15.9
H	6 Micron	332	5037	2247	2.5	17.2
I	6 Micron	337	3263	2025	2.5	14.8
A	6 Micron	360	1073	2247	1.25	11.7
C	6 Micron	338	1754	2247	1.25	14.5
H	6 Micron	332	1954	2247	1.25	15.1
I	6 Micron	337	1103	2025	1.25	12.1
A	SiC 600	360	4806	2247	2.5	17.5
C	SiC 600	338	8567	2247	2.5	22.7
H	SiC 600	332	8817	2247	2.5	22.9
I	SiC 600	338	4946	2025	2.5	18.1

Table 5: Fracture toughness of cemented carbide grades calculated through Hertzian indentation with indenter elastic modulus E' = 700 GPa and Poisson's ratio ν' of indenter is 0.2

TABLE 6

Grade	Kc(RM with β=2)	Kc(RM with β =1.1)	K_{IC}(GGM)
A	11.66	9.62	13.49
B	13.99	11.11	16.30
C	15.29	11.97	17.87
D	12.56	10.21	14.65
E	15.57	12.19	19.52
F	15.34	12.11	19.36
G	16.69	13.00	20.36
H	21.10	16.11	24.36
I	17.76	13.11	21.46

Table 6: Comparison of theoretical fracture toughness models